

Serveur Académique Lausannois SERVAL [serval.unil.ch](http://serval.unil.ch)

## Author Manuscript

Faculty of Biology and Medicine Publication

This paper has been peer-reviewed but does not include the final publisher proof-corrections or journal pagination.

Published in final edited form as:

**Title:** Inhibitory effects of (2S, 3S)-3-[3-[4-(trifluoromethyl)benzoylamino]benzyloxy]aspartate (TFB-TBOA) on the astrocytic sodium responses to glutamate.

**Authors:** Bozzo L, Chatton JY

**Journal:** Brain research

**Year:** 2010 Feb 26

**Issue:** 1316

**Pages:** 27-34

**DOI:** [10.1016/j.brainres.2009.12.028](https://doi.org/10.1016/j.brainres.2009.12.028)

In the absence of a copyright statement, users should assume that standard copyright protection applies, unless the article contains an explicit statement to the contrary. In case of doubt, contact the journal publisher to verify the copyright status of an article.

**Inhibitory effects of (2S, 3S)-3-[3-[4-(trifluoromethyl)benzoylamino]benzyloxy]aspartate (TFB-TBOA) on the astrocytic sodium responses to glutamate**

by

Luigi Bozzo<sup>1,2</sup> and Jean-Yves Chatton<sup>1,2</sup>

<sup>1</sup>Department of Physiology, <sup>2</sup>Department of Cell Biology and Morphology, University of Lausanne, Switzerland

Number of pages: 18

Number of figures: 7

Corresponding author:

Dr. Jean-Yves Chatton, PD MER  
Dept. of Cell Biology and Morphology  
and Dept. of Physiology  
Rue du Bugnon 9

CH-1005 Lausanne  
Switzerland  
Tel: +41-21-692-5106  
Fax: +41-21-692-5105  
E-mail: [jean-yves.chatton@unil.ch](mailto:jean-yves.chatton@unil.ch)

Running title: Glutamate transport inhibition by TFB-TBOA

Abbreviations: GLT-1, glutamate transporter 1; GLAST, glutamate-aspartate transporter; TBOA, DL-*threo*- $\beta$ -benzyloxyaspartate; CNQX, 6-cyano-7-nitroquinoxaline-2,3-dione; I-V, current-voltage; MCPG, (S)- $\alpha$ -Methyl-4-carboxyphenylglycine; EAAT, excitatory amino acid transporter

## Abstract

Astrocytes are responsible for the majority of the clearance of extracellular glutamate released during neuronal activity. DL-*threo*- $\beta$ -benzyloxyaspartate (TBOA) is extensively used as inhibitor of glutamate transport activity, but suffers from relatively low affinity for the transporter. Here, we characterized the effects of (2S, 3S)-3-[3-[4-(trifluoromethyl)benzoylamino]benzyloxy]aspartate (TFB-TBOA), a recently developed inhibitor of the glutamate transporter on mouse cortical astrocytes in primary culture. The glial Na<sup>+</sup>-glutamate transport system is very efficient and its activation by glutamate causes rapid intracellular Na<sup>+</sup> concentration (Na<sup>+</sup><sub>i</sub>) changes that enable real time monitoring of transporter activity. Na<sup>+</sup><sub>i</sub> was monitored by fluorescence microscopy in single astrocytes using the fluorescent Na<sup>+</sup>-sensitive probe sodium-binding benzofuran isophthalate. When applied alone, TFB-TBOA, at a concentration of 1  $\mu$ M, caused small alterations of Na<sup>+</sup><sub>i</sub>. TFB-TBOA inhibited the Na<sup>+</sup><sub>i</sub> response evoked by 200  $\mu$ M glutamate in a concentration-dependent manner with IC<sub>50</sub> value of 43 $\pm$ 9 nM, as measured on the amplitude of the Na<sup>+</sup><sub>i</sub> response. The maximum inhibition of glutamate-evoked Na<sup>+</sup><sub>i</sub> increase by TFB-TBOA was >80%, but was only partly reversible. The residual response persisted in the presence of the AMPA/kainate receptor antagonist CNQX. TFB-TBOA also efficiently inhibited Na<sup>+</sup><sub>i</sub> elevations caused by the application of D-aspartate, a transporter substrate that does not activate non-NMDA ionotropic receptors. TFB-TBOA was found not to influence the membrane properties of cultured cortical neurons recorded in whole-cell patch clamp. Thus, TFB-TBOA, with its high potency and its apparent lack of neuronal effects, appears to be one of the most useful pharmacological tools available so far for studying glial glutamate transporters.

Section: **3.** Neurophysiology, Neuropharmacology and other forms of Intercellular Communication.

Keywords: astrocytes; neurons; glutamate transport inhibition; TBOA; TFB-TBOA, intracellular sodium concentration; ion homeostasis; EAAT

## 1. Introduction

By rapidly taking up extracellular glutamate, astroglial cells play the critical role of protecting neurons from the excitotoxic buildup of glutamate, thereby ensuring the fidelity of glutamatergic transmission at high frequency (Danbolt, 2001). Astrocytic glutamate uptake also plays an important role in the coupling between synaptic activity and glucose utilization, *i.e.* neurometabolic coupling (Pellerin et al., 2007). Astrocytes are equipped with efficient glutamate transporters that surround the synaptic cleft and use the electrochemical gradient of  $\text{Na}^+$  to take up glutamate against its electrochemical gradient. In these cells, the  $\text{Na}^+$ -coupled glutamate transport system is so efficient that the astrocytic intracellular  $\text{Na}^+$  concentration ( $\text{Na}^+_i$ ), undergoes rapid and large elevations when glutamate is applied extracellularly, even at low micromolar concentration (Chatton et al., 2000). The bulk of glutamate uptake in the adult brain is mediated by astroglia that express mostly the excitatory amino acid transporter (EAAT) isoforms 1 and 2, whereas EAAT3 and EAAT4 are considered to be neuronal transporters, and EAAT5 is retina-specific (Danbolt, 2001).

Inhibitors of  $\text{Na}^+$ -dependent glutamate transporters are therefore invaluable tools for elucidating the physiological roles of these transporters in detail. Earlier inhibitors of glutamate transporters, such as *threo*- $\beta$ -hydroxyaspartate (THA) and *trans*-pyrrolidine-2,4-dicarboxylic acid (t-PDC), are transported competitive inhibitors that lead to astrocytic coupled  $\text{Na}^+$  influx (Chatton et al., 2001). A more recently synthesized compound, DL-*threo*- $\beta$ -benzyloxyaspartate (TBOA) has been introduced and since then widely used as a non-transported competitive inhibitor of glutamate transporters (Shimamoto et al., 1998). This compound is a non-selective inhibitor of all EAATs subtypes with activity in the micromolar range. While this compound was a real breakthrough for the study of glutamate transport, its relatively low potency imposes the use of fairly high concentrations, increasing the risk of unwanted effects in particular when used *in situ* (Bernardinelli and Chatton, 2008), or when *in vivo* use is envisaged for instance as a possible treatment for mood disorder pathologies (Lee et al., 2007; Sanacora et al., 2003).

Recently, a series of analogues of TBOA have been reported with both improved potency and selectivity (Shimamoto et al., 2004). Among them, the most promising

one appears to be TFB-TBOA with nanomolar affinity for EAATs. In the present study, we characterized the effects of TFB-TBOA on the  $\text{Na}^+_i$  response to glutamate in primary mouse astrocytes and on the electrical properties of pure cortical neurons in primary culture.

## 2. Results

Glutamate evokes a robust elevation of  $\text{Na}^+_i$  in mouse astrocytes in primary culture (Chatton et al., 2000) that is primarily due to  $\text{Na}^+$ /glutamate cotransport activity. The first set of experiments was aimed at determining whether the new inhibitor of the glutamate transporter TFB-TBOA applied alone influenced baseline  $\text{Na}^+_i$  levels and at characterizing its inhibitory properties on the  $\text{Na}^+_i$  responses to glutamate application.

**Fig. 1A** shows an original experimental trace of the  $\text{Na}^+_i$  response to 200  $\mu\text{M}$  glutamate superfusion in a single astrocyte. In these experiments,  $\text{Na}^+_i$  went from a typical resting value of 12 mM to 33 mM. The baseline  $\text{Na}^+_i$  as well as the amplitude and kinetics of the response to glutamate in this series of experiments corresponds to what was described in previous studies (Chatton et al., 2000).

TFB-TBOA 1  $\mu\text{M}$  was then applied alone leading to a small change in  $\text{Na}^+_i$ . When co-applied with glutamate, TFB-TBOA inhibited  $83\pm 1\%$  of the glutamate response. After washout of TFB-TBOA, the  $\text{Na}^+_i$  response to glutamate was restored however, with a slower kinetics and lower amplitude. **Fig. 1B** summarizes the results obtained in this series of experiments.

An inhibition curve of TFB-TBOA on the astrocytes response to 200  $\mu\text{M}$  glutamate was then established (**Fig. 2**). The graph shows that TFB-TBOA inhibited the  $\text{Na}^+_i$  response with high affinity, with an apparent  $\text{IC}_{50}$  of  $43\pm 9$  nM when measured on the maximal amplitude of the response. In the presence of this maximally effective concentration of TFB-TBOA, about 17% of the  $\text{Na}^+_i$  response to glutamate subsisted (**Figs. 1** and **2**). We thus tested whether this residual response was due to AMPA/kainate receptor activation, which also leads to  $\text{Na}^+_i$  increase in astrocytes (Chatton et al., 2000) rather than to incomplete transporter blockade. **Fig. 3** indicates that co-application of TFB-TBOA and CNQX did not further inhibit the  $\text{Na}^+_i$  response to 200  $\mu\text{M}$  glutamate.

As seen in **Fig. 1**, TFB-TBOA caused a small  $\text{Na}^+_i$  response in the absence of glutamate. We thus tested for the potential involvement of three major classes of astrocytic receptors in this response. **Fig. 3** shows that addition of the AMPA/kainate receptor antagonist CNQX (50  $\mu\text{M}$ ) did not abolish the  $\text{Na}^+_i$  change caused by 1  $\mu\text{M}$  TFB-TBOA. Application of the metabotropic glutamate receptor antagonist (S)- $\alpha$ -Methyl-4-carboxyphenylglycine (MCPG, 1mM) or the P2 purinergic receptor

antagonist suramin (100  $\mu\text{M}$ ) did not influence the response to TFB-TBOA alone, excluding the contribution of these classes of receptors.

In order to have a more direct assessment of the ability of TFB-TBOA to interfere with transport activity, we tested D-aspartate, a substrate of the glutamate transporter that is not metabolized nor activates ionotropic receptors. TFB-TBOA inhibited  $\sim 90\%$  of the  $\text{Na}^+_i$  response to 200  $\mu\text{M}$  D-aspartate in astrocytes (**Fig. 4**). The reversibility of the inhibition on the response to D-aspartate was of  $60 \pm 2\%$ , *i.e.* somewhat lower than was observed with glutamate (see **Fig. 1**).

We then tested whether the incomplete reversibility of the response to glutamate after TFB-TBOA washout was persistent with time. **Fig. 5** indicates that the reversibility improved with time, without however being complete 1 hour after washout of the compound. Interestingly, both the amplitude and the initial rate of  $\text{Na}^+_i$  rise recovered with a similar timecourse.

In order to investigate the mode of action of TFB-TBOA, a Schild analysis was performed (**Fig. 6**). The  $\text{Na}^+_i$  responses to application of glutamate at different concentrations were measured in the absence or in the presence of TFB-TBOA applied at 10, 50 and 100 nM. From a family of three-point dose-response curves, the apparent  $\text{EC}_{50}$  of glutamate was estimated and used to build the Schild plot (**Fig. 6B**), which yielded a linear slope of 1.6 ( $R^2=0.96$ ), different from unity and thus not compatible with pure competitive antagonism.

Finally, we investigated the effect of TFB-TBOA on the membrane properties of cortical neurons in pure primary cultures. Neurons were recorded in whole-cell patch clamp in voltage-clamp configuration and the current-to-voltage relationship was analyzed in the presence and in the absence of 1  $\mu\text{M}$  TFB-TBOA. Current-voltage plot shown in **Fig. 7** shows that the resting membrane potential was -80 mV regardless of the presence or absence of TFB-TBOA and that the inhibitor did not influence the input resistance. In some recorded neurons, spontaneous or network-induced firing of action potentials was observed and did not appear to be influenced by the presence of TFB-TBOA (*not shown*).

### 3. Discussion

The aim of this report was to characterize the effects of the new glutamate transporter inhibitor TFB-TBOA on astrocytes in primary culture. As astrocytes are equipped with a high density of Na<sup>+</sup>-coupled glutamate transporter, Na<sup>+</sup><sub>i</sub> concentration undergoes rapid and robust increases in these cells, which can be measured by microspectrofluorimetric methods (see e.g. Chatton et al., 2000; Rose et al., 1997). This Na<sup>+</sup><sub>i</sub> increase is almost entirely attributable to the activity of the Na<sup>+</sup>-glutamate cotransporters. Glial glutamate transporters use a complex stoichiometry of 3 Na<sup>+</sup> plus 1 H<sup>+</sup> cotransported (or 1 OH<sup>-</sup> exchanged) with 1 glutamate and exchanged against 1 K<sup>+</sup> (Levy et al., 1998). As the transport cycle is electrogenic, glutamate transport leads to a net inward current that can be measured by electrophysiological means. Transport activity can also be measured by radioactive tracers of transporter substrates, e.g. glutamate or D-aspartate. Measuring Na<sup>+</sup><sub>i</sub> changes, as performed in the present study, offers the advantages of assessing transport activity in real time and at the single cell level.

The first non-transported inhibitors of glutamate transporters were dihydrokainate, with selectivity for EAAT2 (GLT-1), and more recently TBOA, acting on all EAAT subtypes. Both compounds have been widely used but suffer from a relatively low affinity on glutamate transporters and are accompanied with complex unwanted effects (Bernardinelli and Chatton, 2008). The newly released compound TFB-TBOA offers the promise of a high potency of inhibition in the nanomolar range.

The original report characterizing TFB-TBOA (Shimamoto et al., 2004) described the inhibition glutamate transport measured by <sup>14</sup>C-glutamate uptake in COS cells expressing EAATs or measured by transporter currents in *Xenopus laevis* oocytes expressing EAATs. The reported IC<sub>50</sub> values were 22, 17 and 300 nM for EAAT1, EAAT2, and EAAT3, respectively.

In the present study TFB-TBOA was tested on mouse astrocytes. The only glutamate transporter functionally expressed in primary mouse astrocytes is the EAAT1 (GLAST) subtype, as the GLT-1 inhibitor dihydrokainate fails to inhibit the Na<sup>+</sup><sub>i</sub> response to glutamate (Chatton et al., 2001). We found that TFB-TBOA inhibited Na<sup>+</sup><sub>i</sub> responses evoked by 200 μM glutamate in a concentration-dependent manner with an apparent IC<sub>50</sub> of 43 nM. Previous measurements of inhibition of synaptically

activated transporter currents in astrocytes in the hippocampus yielded an  $IC_{50}$  value of 13 nM (Tsukada et al., 2005). We found a maximal inhibition of ~80% on the  $Na^+_i$  response to glutamate, whereas the inhibition was more pronounced (~90%) when D-aspartate was used as a transport substrate.

TFB-TBOA showed however incomplete reversibility of inhibition. Whereas the amplitude of the  $Na^+_i$  responses to glutamate measured 5 minutes after washout of the compound was overall 69% of the original amplitude, the rise-time was significantly slower (~4-fold), possibly because some fraction of the compound remains bound because of its high affinity for the transporter. It is plausible that TFB-TBOA does not only act as a pure competitive inhibitor of transport, but also displays some non-competitive component. Schild analysis of the inhibition of glutamate-mediated  $Na^+_i$  responses by TFB-TBOA indeed supported this conclusion. In addition, we observed that reversibility of responses was gradually improving with time after washout of the drug. This result is consistent with observations made on EAAT transporter currents measured in oocytes (Shimamoto et al., 2004), for which the recovery was incomplete even 1 hour after washout of TFB-TBOA. We found that not only did the amplitude gradually recovered, but also the initial rate of  $Na^+_i$  rise with a similar timecourse. Our previous mathematical modeling of the  $Na^+_i$  response to glutamate has shown that this parameter best reflects the kinetics properties of the transporter (Chatton et al., 2000). This indicates that TFB-TBOA causes an alteration of transporter function, which persists after washout of the drug. This incomplete reversibility of inhibition is a limitation for the use of TFB-TBOA that has to be taken into account in experimental designs.

Whereas TFB-TBOA applied alone was shown not to elicit detectable currents in oocytes expressing glutamate transporters (Shimamoto et al., 2004), we found, however, that in primary mouse astrocytes a small but significant  $Na^+_i$  increase was evoked by TFB-TBOA, as was found to be the case for TBOA (Chatton et al., 2001). As NMDA receptors are not found in cultured astrocytes (Verkhratsky and Kirchhoff, 2007) and as the AMPA/kainate receptor antagonist CNQX did not prevent this  $Na^+_i$  increase, the mechanism of the TFB-TBOA evoked  $Na^+_i$  rise does not involve ionotropic glutamate receptors. Metabotropic glutamate and P2 purinergic receptors could also be excluded. Thus, this response to TFB-TBOA could be related to interference with other  $Na^+$  carrier proteins such as the  $Na,K$ -ATPase. The

observation would also be compatible with TFB-TBOA being a low efficacy transporter substrate, which could elicit a small  $\text{Na}^+$  response.

In previous studies performed under the same experimental conditions, we had found that the maximum inhibition caused by TBOA on the  $\text{Na}^+$  response to 200  $\mu\text{M}$  glutamate was ~70% (Chatton et al., 2001). We show here that the maximal inhibition caused by TFB-TBOA on the response to glutamate was somewhat larger (>80%). As was found for TBOA, the TFB-TBOA-insensitive residual  $\text{Na}^+$  response to glutamate, was not mediated by non-NMDA receptors and it is currently unclear what pathways is responsible for this residual signal. By contrast, the EAAT transporter currents measured in oocytes were reported to be fully inhibited by TFB-TBOA (Shimamoto et al., 2004).

It is generally accepted that astroglial cells *in situ* express mostly the EAAT2 (GLT-1) subtype of transporter (Dunlop, 2006), whereas when studied in primary cultures, EAAT1 (GLAST) becomes the almost exclusively functional isoform expressed. As was the case with TBOA, TFB-TBOA has almost identical affinity for both isoforms of the transporter (Shimamoto et al., 2004). However, TFB-TBOA was reported to have an approximately 15-fold lower affinity for EAAT3, a mostly neuronal transporter isoform, which means that this compound could potentially be used to discriminate between the contribution of glial and neuronal glutamate transport in the intact tissue. In addition, we found that TFB-TBOA at its maximally effective concentration did not influence the passive membrane electrical properties of cortical neurons and apparently did not alter their excitability.

Selective inhibition of the EAAT2 (GLT-1) subtype is classically achieved with dihydrokainate, which, however, possesses a fairly low affinity for the transporter (Bridges and Esslinger, 2005) and causes complex effects on astrocytes *in situ* (Bernardinelli and Chatton, 2008). A very recent report described the first selective inhibitor of EAAT1, UCPH-101, with an  $\text{IC}_{50}$  of ~1  $\mu\text{M}$  and > 400-fold selectivity over EAAT2 and EAAT3 (Jensen et al., 2009). With TFB-TBOA acting on both glial isoforms, the latter pharmacological tool could represent an interesting complement for the functional studies of glutamate transport.

Taken together, the present study showed that TFB-TBOA is able to inhibit  $\text{Na}^+$ -dependent glutamate transport in astrocytes with high potency. Despite a partial

reversibility of inhibitory effects that have to be taken into account in experimental designs, TFB-TBOA is to be considered as an extremely valuable tool to study glutamate transport and neuron-glia interactions.

## 4. Experimental Procedure

### 4.1. Cell culture and solutions

Every effort was made to minimize suffering and the number of animals used in all experiments. In addition, all the procedures used to prepare living cells have been approved by the Swiss legislation and follows their guidelines. Primary cultures of mouse astrocytes were prepared as previously described (Chatton et al., 2000). After microdissection of cortices from 1-4 days-old C57bl6 mice, tissue was mechanically dissociated by successive aspirations through sterile syringes. The isolated astrocytes were then plated on glass coverslips and cultured in DME medium (D7777, Sigma, Buchs, Switzerland) supplemented with 10% FCS penicillin, streptomycin and amphotericin. Astrocytes were used after 2-3 weeks of culture.

Mouse cortical neurons in primary cultures were obtained from 17-days C57bl6 mouse embryos. After removing meninges, entire cortices were first incubated with 20 U/ml papain for 30 min at 34°C and then mechanically dissociated in MEM medium plus glucose, glutamine and 10% FCS, by successive aspiration through sterile plastic 2 ml pipettes. The dissociated cells were centrifuged at 1300 rpm for 2 minutes and then re-suspended at a density of 80-85,000 cells per cm<sup>2</sup> in Neurobasal (Invitrogen, Basel, Switzerland) culture medium complemented with 2% B27 solution (Invitrogen), 500 µM glutamine according to Brewer et al. (Brewer et al., 1993). Cells were then plated on glass coverslips coated with poly-L-Ornithine (Sigma, Buchs, Switzerland). Cells were used after 7-14 days of culture.

Experimental solutions used during experiments with astrocytes and neurons contained (mM): NaCl 135, KCl 5.4, NaHCO<sub>3</sub> 25, CaCl<sub>2</sub> 1.3, MgSO<sub>4</sub> 0.8, NaH<sub>2</sub>PO<sub>4</sub> 0.78, glucose 5, bubbled with 5% CO<sub>2</sub>/95% air.

TBOA and TFB-TBOA were from Tocris-Anawa Trading (Zürich). Unless otherwise state, all other compounds were from Sigma.

### 4.2 Na<sup>+</sup><sub>i</sub> fluorescence imaging

Na<sup>+</sup><sub>i</sub> measurements were performed as previously described (Chatton et al., 2000). Briefly, experiments were carried out on the stage of an inverted epifluorescence microscope (Nikon, Tokyo, Japan) and observed through a 40x 1.3 N.A. oil-

immersion objective lens (Nikon). Fluorescence excitation wavelengths were selected using fast filter wheel (Sutter Instr., Novato, CA) and fluorescence was detected using a Gen III+ intensified CCD camera (VideoScope Intl., Washington D.C.). Acquisition and digitization of video images, as well as time series was computer-controlled using the software Metafluor (Universal Imaging, West Chester, PA, USA) running on a Pentium computer. Four video frames were averaged at each wavelength and the acquisition rate of ratio images was varied between 0.5 Hz and 0.1 Hz. Up to 10 individual astrocytes were simultaneously analyzed in the selected field of view.

$\text{Na}^+_i$  was measured in single cells grown on glass coverslips after loading the cells with the  $\text{Na}^+$ -sensitive fluorescent dye sodium-binding benzofuran isophthalate (SBFI-AM, Teflabs, Austin, TX). Cell loading was performed at 37°C using 15  $\mu\text{M}$  SBFI-AM in a HEPES-buffered balanced solution containing (mM): NaCl 160, KCl 5.4, HEPES 20,  $\text{CaCl}_2$  1.3,  $\text{MgSO}_4$  0.8,  $\text{NaH}_2\text{PO}_4$  0.78, glucose 20 and was supplemented with 0.1 % Pluronic F-127 (Molecular Probes, Eugene, OR).

Once loaded with SBFI, cells were placed in a thermostated perfusion chamber designed for rapid exchange of perfusion solutions and superfused at 35°C. Fluorescence was sequentially excited at 340 nm and 380 nm and detected at  $>520$  nm. Fluorescence excitation ratios ( $F_{340\text{nm}}/F_{380\text{nm}}$ ) were computed for each image pixel and produced ratio-images of cells that were proportional with  $\text{Na}^+_i$ . *In situ* calibration was performed after each experiment by permeabilization of the cell membrane for monovalent cations using 6  $\mu\text{g}/\text{ml}$  gramicidin and 10  $\mu\text{M}$  monensin with simultaneous inhibition the  $\text{Na}^+/\text{K}^+$ -ATPase using 1 mM ouabain. Cells were then sequentially perfused with solutions buffered at pH 7.2 with 20 mM HEPES and containing 0, 10, 20 and 50 mM  $\text{Na}^+$ , respectively, and 30 mM  $\text{Cl}^-$ , 136 mM gluconate with a constant total concentration of  $\text{Na}^+$  and  $\text{K}^+$  of 165 mM. A four-point calibration curve was computed for each selected cell in the field of view and used to convert fluorescence ratio values ( $F_{340\text{nm}}/F_{380\text{nm}}$ ) into  $\text{Na}^+$  concentrations.

#### 4.3. Whole-cell electrophysiological recordings in neurons

Whole-cell voltage-clamp recordings were made with borosilicate glass pipettes with a resistance of 5.5-8 M $\Omega$ . In voltage-clamp mode, the clamp potential was set at -70 mV. Recordings were made with an Axopatch 200A amplifier (Axon Instruments).

Current were filtered at 1 kHz. Data were acquired with a Digidata 1440A (Axon), at 10 kHz sampling rate, controlled with Pclamp 10 software and analyzed with Clampfit software (Axon). A period of 5 min was routinely allowed after establishment of the whole-cell configuration. The patch-clamp intracellular solution contained (in mM): K-gluconate 130, NaCl 5, Na-phosphocreatine 10, MgCl<sub>2</sub> 1, EGTA 0.02, HEPES 10, Mg-ATP 2, Na<sub>3</sub>-GTP 0.5, pH 7.3 (adjusted with KOH).

Experiments were performed using an open perfusion chamber. Control extracellular solutions and solutions containing the tested drugs were gravity fed at 600 µl/min and 35°C on the cultured cells.

#### 4.4. Data analysis

Data are means ± SEM and are represented as percentage of the control current or voltage amplitude. Paired student t-tests or ANOVA tests were performed to assess the statistical significance (\*, P<0.05; \*\*, P≤0.01). The half-maximum inhibitory concentration (IC<sub>50</sub>) of TFB-TBOA on the response to glutamate was determined by non-linear curve fitting performed using the Levenberg-Marquardt algorithm implemented in the Kaleidagraph software package (Synergy Software, Reading, PA, USA). The dose-response analysis experiments were fitted using the following equation:

$$R_{obs} = R_{max} [I] / (K + [I]) + R_{min} \quad (1)$$

where  $R_{obs}$ , is the observed response,  $R_{max}$ ,  $R_{min}$  are maximum and minimum parameters of the response.  $[I]$  is the concentration of the inhibitor compound and  $K$  the concentration that yields its half-maximum inhibition (*i.e.* IC<sub>50</sub>).

## **Acknowledgments**

We gratefully acknowledge Guillaume Azarias, Christophe Lamy, and Anita Luthi for their comments of the manuscript and Steeve Menetrey for his excellent technical assistance. This study was supported by grant #3100A0-119827 from the Swiss National Science Foundation to JY Chatton.

## References

- Bernardinelli, Y., Chatton, J.-Y., 2008. Differential effects of glutamate transporter inhibitors on the global electrophysiological response of astrocytes to neuronal stimulation. *Brain Research*. 1240, 47-53.
- Bridges, R. J., Esslinger, C. S., 2005. The excitatory amino acid transporters: pharmacological insights on substrate and inhibitor specificity of the EAAT subtypes. *Pharmacology & Therapeutics*. 107, 271-85.
- Chatton, J.-Y., Marquet, P., Magistretti, P. J., 2000. A quantitative analysis of L-glutamate-regulated Na<sup>+</sup> dynamics in mouse cortical astrocytes: implications for cellular bioenergetics. *European Journal of Neuroscience*. 12, 3843-3853.
- Chatton, J.-Y., Shimamoto, K., Magistretti, P. J., 2001. Effects of glial glutamate transporter inhibitors on intracellular Na<sup>+</sup> in mouse astrocytes. *Brain Research*. 893, 46-52.
- Danbolt, N. C., 2001. Glutamate uptake. *Progresses in Neurobiology*. 65, 1-105.
- Dunlop, J., 2006. Glutamate-based therapeutic approaches: targeting the glutamate transport system. *Curr Opin Pharmacol*. 6, 103-7.
- Jensen, A. A., Erichsen, M. N., Nielsen, C. W., Stensbol, T. B., Kehler, J., Bunch, L., 2009. Discovery of the First Selective Inhibitor of Excitatory Amino Acid Transporter Subtype 1. *Journal of Medicinal Chemistry*. 52, 912–915.
- Lee, Y., Gaskins, D., Anand, A., Shekhar, A., 2007. Glia mechanisms in mood regulation: a novel model of mood disorders. *Psychopharmacology (Berl)*. 191, 55-65.
- Levy, L. M., Warr, O., Attwell, D., 1998. Stoichiometry of the glial glutamate transporter GLT-1 expressed inducibly in a Chinese hamster ovary cell line selected for low endogenous Na<sup>+</sup>-dependent glutamate uptake. *Journal of Neuroscience*. 18, 9620-9628.
- Pellerin, L., Bouzier-Sore, A. K., Aubert, A., Serres, S., Merle, M., Costalat, R., Magistretti, P. J., 2007. Activity-dependent regulation of energy metabolism by astrocytes: An update. *Glia*. 55, 1251-1262.
- Rose, C. R., Ransom, B. R., Waxman, S. G., 1997. Pharmacological characterization of Na<sup>+</sup> influx via voltage-gated Na<sup>+</sup> channels in spinal cord astrocytes. *Journal of Neurophysiology*. 78, 3249-3258.

Sanacora, G., Rothman, D. L., Mason, G., Krystal, J. H., 2003. Clinical studies implementing glutamate neurotransmission in mood disorders. *Annals of the New York Academy of Sciences*. 1003, 292-308.

Shimamoto, K., Lebrun, B., Yasuda-Kamatani, Y., Sakaitani, M., Shigeri, Y., Yumoto, N., Nakajima, T., 1998. DL-threo-beta-benzyloxyaspartate, a potent blocker of excitatory amino acid transporters. *Molecular Pharmacology*. 53, 195-201.

Shimamoto, K., Sakai, R., Takaoka, K., Yumoto, N., Nakajima, T., Amara, S. G., Shigeri, Y., 2004. Characterization of novel L-threo-beta-benzyloxyaspartate derivatives, potent blockers of the glutamate transporters. *Molecular Pharmacology*. 65, 1008-15.

Tsukada, S., Iino, M., Takayasu, Y., Shimamoto, K., Ozawa, S., 2005. Effects of a novel glutamate transporter blocker, (2S, 3S)-3-[3-[4-(trifluoromethyl)benzoylamino]benzyloxy]aspartate (TFB-TBOA), on activities of hippocampal neurons. *Neuropharmacology*. 48, 479-91.

Verkhatsky, A., Kirchhoff, F., 2007. NMDA Receptors in glia. *Neuroscientist*. 13, 28-37.

## Figure legends

Fig. 1 – Inhibition by TFB-TBOA of the glutamate-evoked  $\text{Na}^+_i$  response. (A) representative experimental trace depicting the  $\text{Na}^+_i$  increase caused by application of 200  $\mu\text{M}$  glutamate followed by the application of TFB-TBOA 1  $\mu\text{M}$  alone and subsequently applied with glutamate. A final application of glutamate shows the reversibility of the response. (B) TFB-TBOA effects on the glutamate-evoked  $\text{Na}^+_i$  response. Results are expressed as maximum amplitude of  $\text{Na}^+_i$  and presented as percent of those observed with 200  $\mu\text{M}$  glutamate. Data are means  $\pm$  SEM of 40 cells from 5 independent experiments.

Fig. 2 – Concentration-dependency of the inhibitory effects of TFB-TBOA. Inhibitory curve on the maximum amplitude of  $\text{Na}^+_i$  response to 200  $\mu\text{M}$  glutamate. Non-linear least square fits using 135 cells from 17 experiments yielded  $\text{IC}_{50}$  values of  $43 \pm 9$  nM. The maximum inhibition was observed at 1  $\mu\text{M}$  TFB-TBOA.

Fig. 3 – Residual  $\text{Na}^+_i$  increase in the presence of TFB-TBOA. The TFB-TBOA-insensitive residual  $\text{Na}^+_i$  response to 200  $\mu\text{M}$  glutamate was not altered by non-NMDA receptor inhibitor CNQX (50  $\mu\text{M}$ , means  $\pm$  SEM of 40 cells from 5 independent experiments). The  $\text{Na}^+_i$  increases observed upon TFB-TBOA (1  $\mu\text{M}$ ) application alone were not abolished by non-NMDA receptor inhibitor CNQX (50  $\mu\text{M}$ , 52 cells from 7 independent experiments), the metabotropic glutamate receptor antagonist MCPG (1 mM, 40 cells from 5 experiments), or the P2 purinergic receptor antagonist suramin (100  $\mu\text{M}$ , 23 cells from 3 experiments). Results are expressed as maximum amplitude of  $\text{Na}^+_i$  and presented as percent of those observed with 200  $\mu\text{M}$  glutamate used as a control.

Fig. 4 – Inhibition by TFB-TBOA of the D-aspartate-evoked  $\text{Na}^+_i$  response. Results are expressed as maximum amplitude of  $\text{Na}^+_i$  and presented as percent of those observed with 200  $\mu\text{M}$  D-aspartate. Data are means  $\pm$  SEM of 56 cells from 7 independent experiments.

**Fig. 5** – Reversibility of TFB-TBOA inhibitory effects. The recovery of the response to 200  $\mu\text{M}$  glutamate was tested consecutively 5, 15, 30, 60 minutes after washout of TFB-TBOA (1  $\mu\text{M}$ ). Results are expressed as amplitude or initial rate of rise of  $\text{Na}^+_i$  responses and presented as percent of the response recorded for the first control application of 200  $\mu\text{M}$  glutamate. The significance of recovery was tested against the initial control glutamate application. Data are means  $\pm$  SEM of 46 cells from 6 independent experiments.

**Fig. 6** – Schild analysis of inhibitory action of TFB-TBOA. **(A)** The  $\text{Na}^+_i$  responses to applications of glutamate at different concentrations were measured in the absence or in the presence of TFB-TBOA present at three different concentrations indicated in the graph. Data are means  $\pm$  SEM of 16-24 cells from 13 experiments. **(B)** Schild plot of the data in (A). Dose ratio is the ratio of the apparent  $\text{EC}_{50}$  of glutamate obtained from the family of three-point dose-response curves in (A) in the presence of a given concentration of TFB-TBOA over the  $\text{EC}_{50}$  of glutamate in the absence of TFB-TBOA. The linear regression yielded a slope of 1.6 ( $R^2=0.96$ ).

**Fig. 7** – Effects of TFB-TBOA on the passive membrane properties of cultured cortical neurons in whole-cell configuration. **(A)** Representative whole-cell current responses of a neuron to 20 mV voltage steps (-140 mV to -60 mV, see *inset*). The cell was clamped at -70 mV and measurements were done with and without 1  $\mu\text{M}$  TFB-TBOA. **(B)** Current-voltage relationship recorded in the absence and in the presence of TFB-TBOA, as well as after washout of the compound. Input resistances were not significantly different among groups. Data are means  $\pm$  SEM from 9 individually recorded neurons.

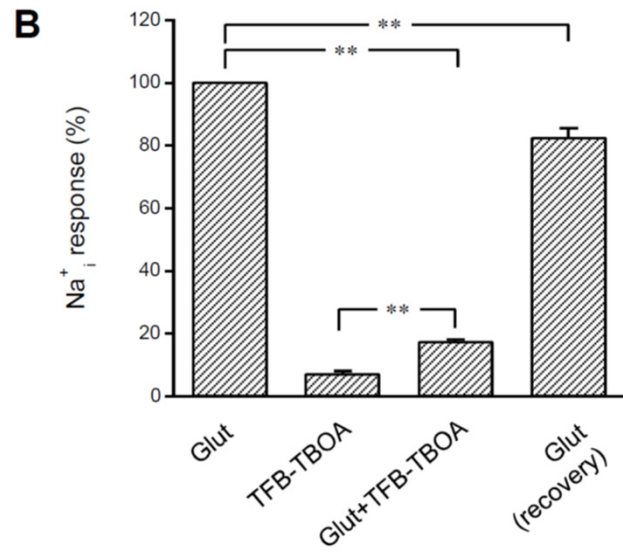
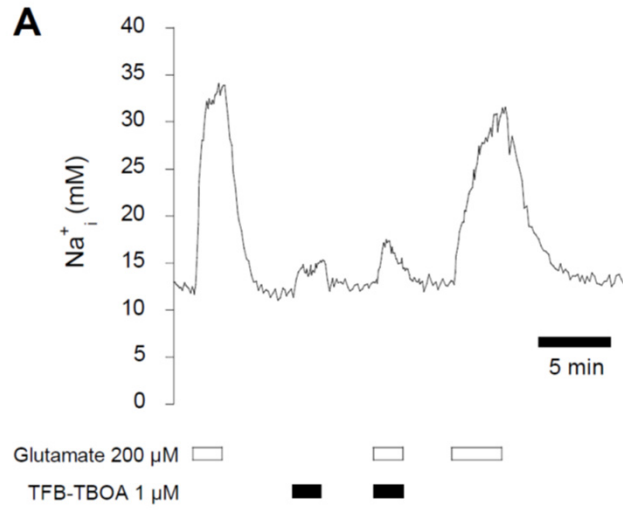


Figure 1

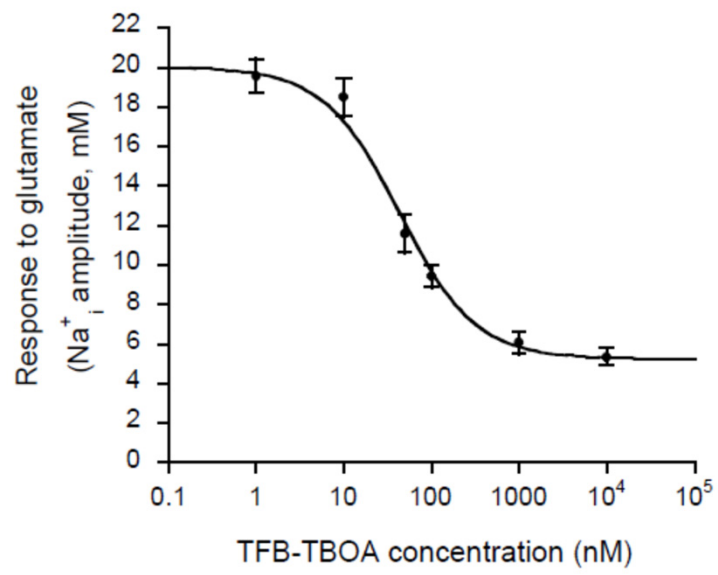


Figure 2

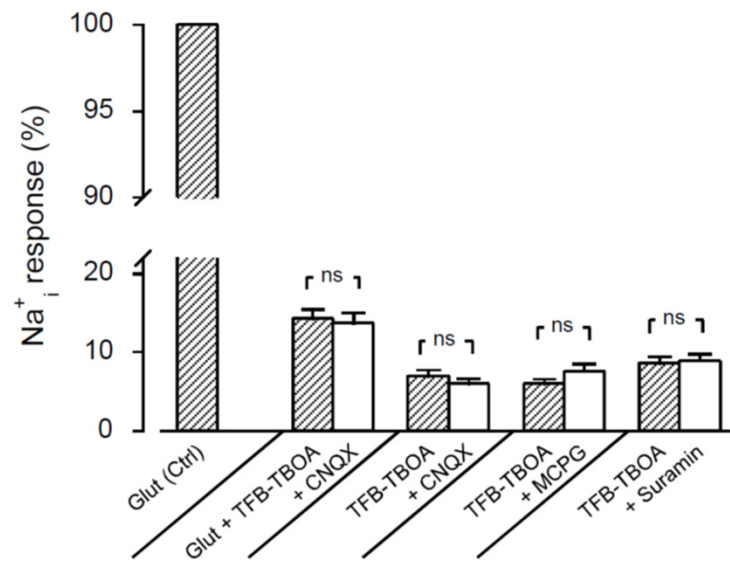


Figure 3

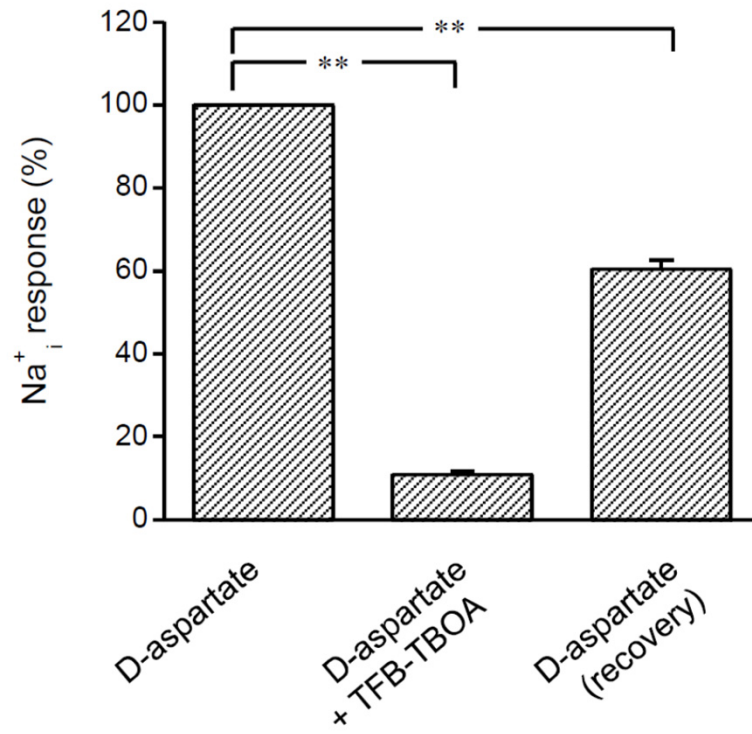


Figure 4

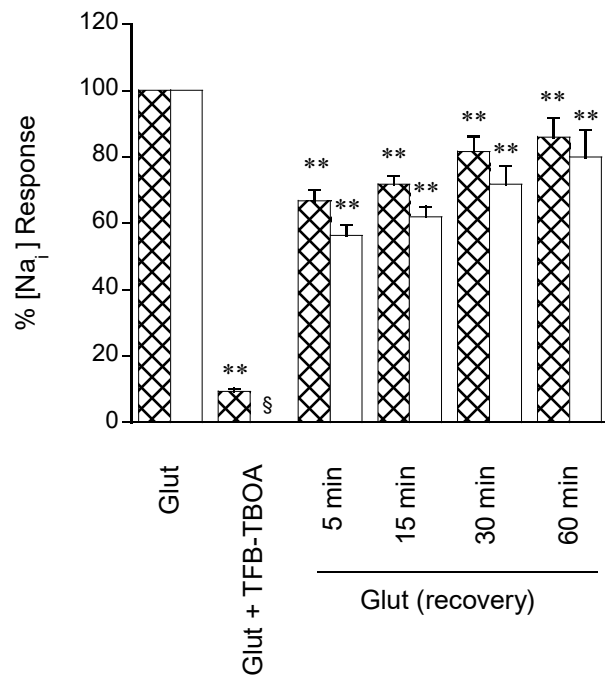


Figure 5

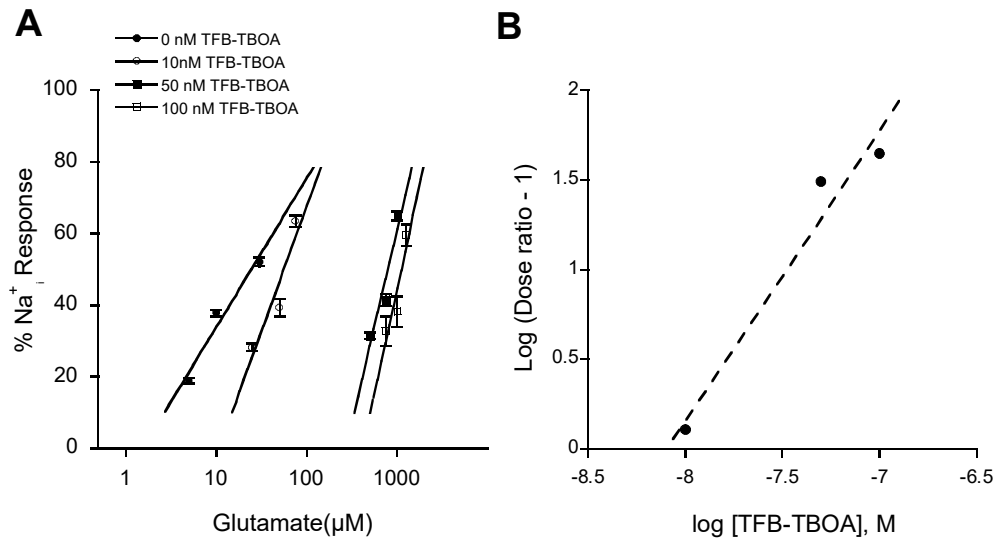


Figure 6

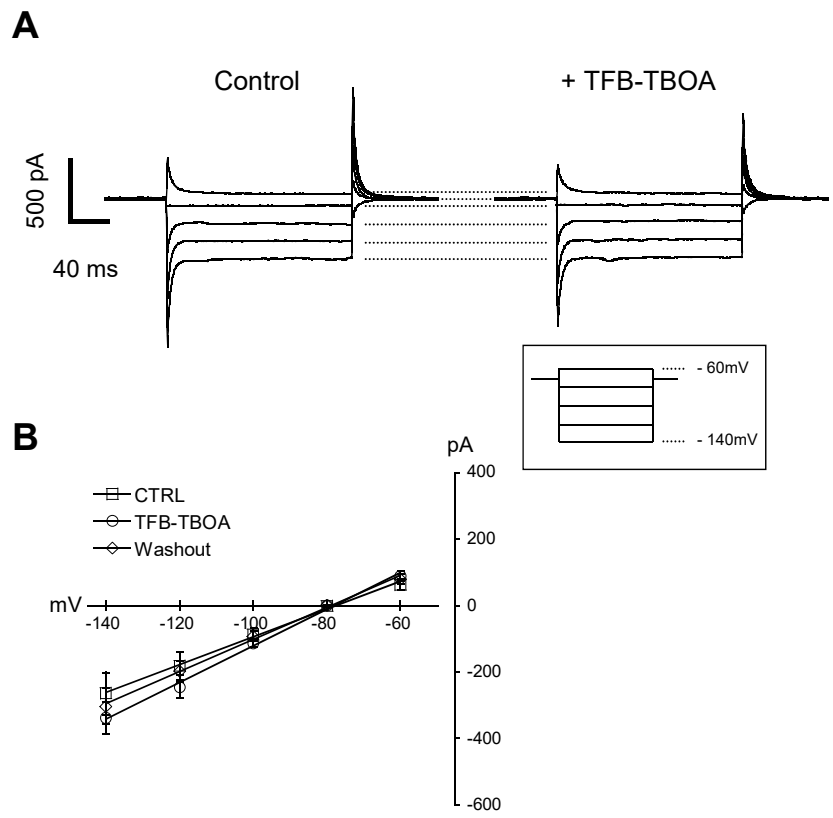


Figure 7